International Journal of Structural Stability and Dynamics
Vol. 19, No. 8 (2019) 1950098 (30 pages)

DOI: 10.1142/S0219455419500986

Improved Generalized Procedure for Determining Critical State of a Thin-Walled Beam Under Combined Symmetric Loads

Phung Van Binh*, Nguyen Viet Duc†, Prokopov Vladimir Sergeevich‡ and Dang Hoang Minh§,¶,‖

*Faculty of Aerospace Engineering
Le Quy Don Technical University
Hanoi, Vietnam

†Faculty of Civil Engineering
Thuyloi University
175 Tay Son, Dong Da, Hanoi, Vietnam

‡Bauman Moscow State Technical University
Moscow, Russian Federation

§Division of Construction Computation
Institute for Computational Science
Ton Duc Thang University
Ho Chi Minh City, Vietnam

¶Faculty of Civil Engineering
Ton Duc Thang University
Ho Chi Minh City, Vietnam
‖danghoangminh@tdtu.edu.vn

Received 8 December 2018
Accepted 2 May 2019
Published 18 June 2019

This paper presents an improved generalized procedure for dealing with the stability of thin-walled beams under combined symmetric loads based on the energy method. The differential equations for the case of complex loading conditions were developed using an axis transformation matrix. The work caused by external loads was related to the work of internal forces to simplify the computational procedure. The thin-walled beam subjected to axial force F, bending moment M at both ends, and concentrated load P at midspan was studied. The case of a concentrated load P replaced by a distributed load q over partial beam length was also examined. The stability region boundary of the beam was derived by two approaches: one was to estimate an approximate angle of twist prior to determination of the deflection and the other was to do it in the reverse way. Numerical results reveal that the first approach yields less error than the second; however, the outcome obtained by the former was more cumbersome than the

‖Corresponding author.

latter. Above all, both approaches provided feasible results and are useful for further applications dealing with the stability analysis of thin-walled beams.

Keywords: Thin-walled beam; stability analysis; stability region; symmetric load; energy method.

1. Introduction

Thin-walled beams have been used widely in mechanical engineering, civil engineering, aviation, and others.[1–7] In practice, it was observed that they were often subjected to different types of loading simultaneously, as well as within different boundary conditions yielded from diverse installation manners in each structure.[8–13] On the one hand, stability analysis of those beams, based on system of differential equations, frequently turned out to be intricate and most of the time there was no exact solution.[14] On the other hand, computer-aided engineering (CAE) softwares, based on the finite element method (FEM), only provided the analysis in a "one-way" direction.[15–20] As an example, if there is a beam subjected to a complex loading system including distributed load q, axial force F, and bending moment M at both ends, CAE softwares are able to provide stability safety factor only if there are input data of q, F, and M, but it seems to be useless for the inverse analysis, such as if there are input data of q and M, which value of F will bring the system into the unstable state? The up-to-date CAE softwares cannot answer this question in such type of analysis. Therefore, the development of explicit (precise) analytical expressions to evaluate the beam state under complex loading system corresponding to different boundary conditions is truly indispensable.

Stability issues of thin-walled beams under individual load such as F, M, q or concentrated load P were described in detail in the works of Timoshenko and Gere,[1] Vlasov,[2] Alfutov,[3] Bazant and Cedolin,[4] and Kim *et al.*[5] Yet, Chen *et al.*[6] also proposed an approach to calculation of critical lateral-torsional buckling loads of beams subjected to transverse loads; particularly in order to make the calculation process simpler, the externally applied loads have been evaluated by using the internal bending moment and internal shear force. On one side, stability issues of the beams subjected to two types of loading have been paid a special attention and studied lately by many researchers such as Leung,[13] Chu *et al.*,[14] Mohri *et al.*,[21,22] Cheng *et al.*,[23] and Yilmaz and Kirac.[24] On the other side, few studies on the stability state of the beams subjected to three and more types of loading, including the works of Papkovitch,[25] Magnucka-Blandzi,[26,27] Osmani and Meftah,[28] have been found in the literature.

In particular, Phung *et al.*[29] have recently obtained several analytical expressions from the stability analysis of thin-walled beams subjected to three types of loading such as M, q, and F. Besides, the analytical expression describing the boundary surface of stability region of the beam was derived and illustrated visually in the space of M-q-F. Although the obtained results were quite useful for practical calculations in dealing with the stability issues of the beams, only the case of uniformly

distributed load q above the full beam length was considered. In fact, there are many cases that load q is only distributed in partial beam length; however, in such cases, the stability issue has not been studied yet.

Regarding the combined loading condition, the difficulty is not only how to solve the system of differential equations, but also how to develop this system because the generalized system of diferential equations describing critical state needs to start at the local coordination $O\xi\eta\zeta$ (Fig. 1). However, the system starting right at the global coordination $Oxyz$, automatically eliminating minor components, has been found in most of published work so far. This fact not only results in solution incorrectness, but also it causes obscurity and reader's misunderstanding.

From literature review on thin-walled beams, several matters are still questionable as follows: (i) How can the generalized system of differential equations for stability problem of the beams subjected to combined loading condition be developed? (ii) How can stability region be analyzed if load q is applied only over part of beam length? (iii) How does the application height of uniform distributed load q influence on the stability state of the system? (iv) If uniform distributed load q is replaced by concentrated load P at the beam center, how will the stability state of the beams under loading system of M-P-F be affected? (v) Is there any possibility to develop generalized expressions for both cases of load q and load P?

In this paper, a generalized procedure is proposed to deal with the stability issue of the thin-walled beam under symmetric combined external loads. The most important steps to develop the system of differential equations are explained by using the axis transformation matrix $[K]$. This point distinguishes among other published works. By using the same problem-solving approach, two cases are considered; the first one (Fig. 1) is a thin-walled beam subjected to force F, moment M, and load P. While load q replaces load P in the second case (Fig. 5), however, load q in this work is considered in a generalized form, i.e. partial distributed load. Besides, the remarkable point here is that based on the expression describing the boundary surface of stability region at the second case, it is possible to yield the results for the case when q is distributed in the full beam length as well as when load q is replaced by load P at the beam center. Load P or q application height's affect on the stability state of the system is also studied. Yet, the method for defining work caused by external loads through work of internal force is suggested in this work in order to make the computational process smoothly. Likewise, the stability region boundary of the system is represented not only by algebraic equations, but also by a graphical form in the space of different load parameters. Hence, the equations could support the manufacturer to verify the stability issue of the beams, besides they might also be used properly for optimal design of the beam with lateral-torsional buckling constraints.[30,31]

2. Generalized Procedure and Fundamental Equations

As stated before, a simply supported thin-walled beam of length L and with doubly symmetric cross-sections subjected to combined external loads is considered in this

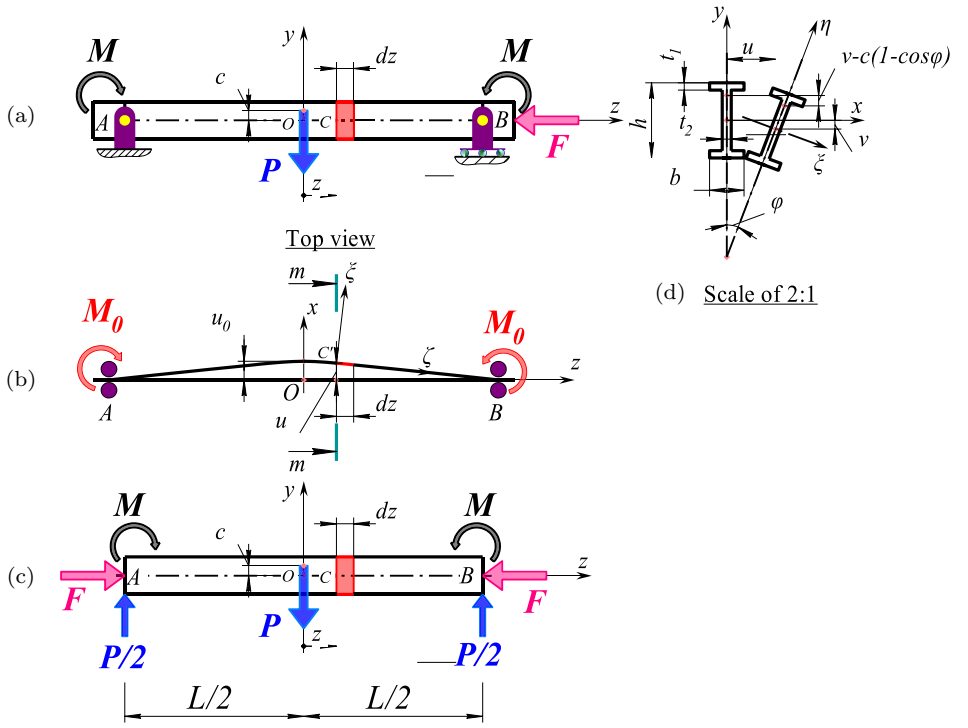

Fig. 1. Scheme of the beam under combined loads *M-P-F*.

work. The external load system is symmetric, as illustrated in Figs. 1 and 5 for the first and second cases, respectively. Apart from the principal coordinate system *Oxyz*, which is situated at the gravity center of the central cross-section, there is an auxiliary one $O\xi\eta\zeta$ associated with the cross-section in a deformed state. Symbols u and v are considered as deflections in x and y directions, respectively, while M_x, M_y, M_z, M_ξ, M_η, M_ζ are denoted as moments acting on the corresponding axes. The angle of twist and deflections of the beam cross-section are considered to be insignificant. For the sake of external load symmetry, the beam is divided into two equal parts, and the equation of equilibrium is just established for the right one (segment *OB* in Figs. 1 and 5). Also, the generalized procedure is described in Fig. 2 and explained in detail subsequently.

Step 1: *Development of formulae for internal moments* M_x, M_y, M_z *at beam cross-section in the global coordination Oxyz.*

Based on the boundary condition and external loads, the internal moments M_x, M_y, M_z within the global coordination *Oxyz* are defined by using strength of materials theory. This is one of the most important steps to develop the system of differential equations correctly.

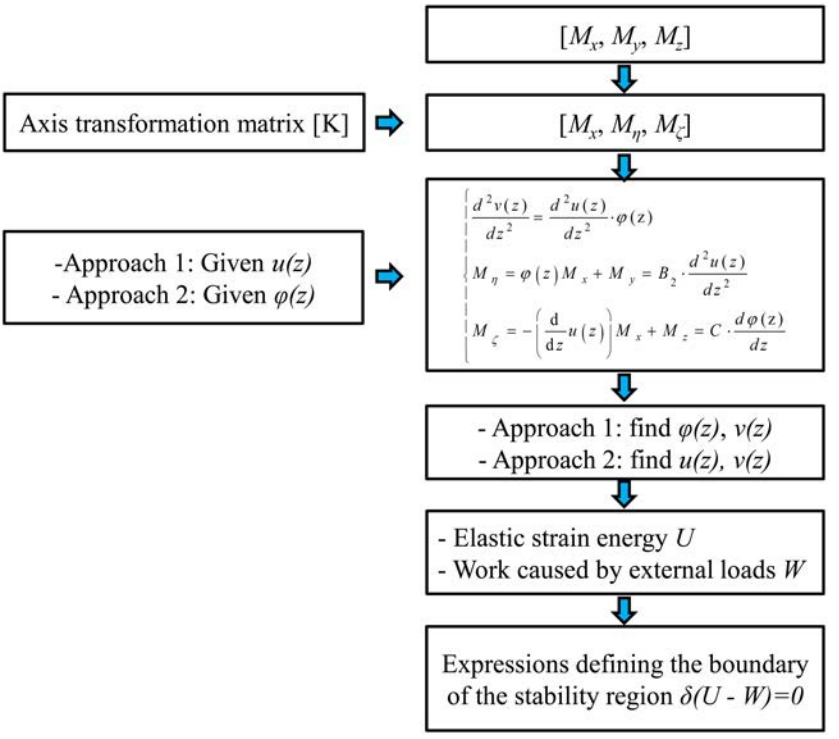

Fig. 2. Generalized procedure for stability analysis of thin-walled beams under combined loads.

Step 2: *Determination of axis transformation matrix* $[K]$

The matrix $[K]$, correlating the global coordination $Oxyz$ with the local $O\xi\eta\zeta$, needs to be defined properly. For the coordination of structural system described in Fig. 1 and Fig. 5, the matrix $[K]$ is as follows:

$$[K] = \begin{bmatrix} 1 & -\varphi(z) & \dfrac{d}{dz}u(z) \\ \varphi(z) & 1 & \dfrac{d}{dz}v(z) \\ -\dfrac{d}{dz}u(z) & -\dfrac{d}{dz}v(z) & 1 \end{bmatrix}. \tag{1}$$

Step 3: *Development of formula for internal moments* M_ξ, M_η, M_ζ *at beam cross-section in the local coordination* $O\,\xi\eta\zeta$

Internal moments M_ξ, M_η, M_ζ are determined in accordance with M_x, M_y, M_z based on axis transformation matrix $[K]$:

$$\begin{bmatrix} M_\xi \\ M_\eta \\ M_\zeta \end{bmatrix} = [K]\cdot\begin{bmatrix} M_x \\ M_y \\ M_z \end{bmatrix}. \tag{2}$$

Substituting the matrix $[K]$ from Eq. (1) into Eq. (2), it results in:

$$\begin{bmatrix} M_\xi \\ M_\eta \\ M_\zeta \end{bmatrix} = \begin{bmatrix} M_x - \varphi \cdot M_y + \left(\dfrac{d}{dz}u\right) M_z \\ \varphi \cdot M_x + M_y + \left(\dfrac{d}{dz}v\right) M_z \\ -\left(\dfrac{d}{dz}u\right) M_x - \left(\dfrac{d}{dz}v\right) M_y + M_z \end{bmatrix}. \tag{3}$$

For thin-walled beams, the deflection v and the slope d/dz^v (those cause flexural mode), which are very small, do not interact with the lateral-torsional buckling, hence the elements containing d/dz^v in Eq. (3) can be omitted.[1,29] Thus, internal moments $[M_\xi, M_\eta, M_\zeta]$ are approximated as follows:

$$\begin{bmatrix} M_\xi \\ M_\eta \\ M_\zeta \end{bmatrix} = \begin{bmatrix} M_x - \varphi \cdot M_y + \left(\dfrac{d}{dz}u\right) \cdot M_z \\ \varphi \cdot M_x + M_y \\ -\left(\dfrac{d}{dz}u\right) \cdot M_x + M_z \end{bmatrix}. \tag{4}$$

Step 4: *Development of the system of differential equations associated with the global coordination Oxyz*

Beginning with the system of differential equations describing the critical state of beam associated with the local coordination $O\xi\eta\zeta$, it is illustrated in the general form as follows[1,2,29]:

$$M_\xi = B_1 \frac{d^2 v}{dz^2}, \tag{5}$$

$$M_\eta = B_2 \frac{d^2 u}{dz^2}, \tag{6}$$

$$M_\zeta = C \frac{d\varphi}{dz} - DD \frac{d^3 \varphi}{dz^3}. \tag{7}$$

Taking into account that C is torsional stiffness, $B_1 = EJ_1$ is the maximum bending stiffness, $B_2 = EJ_2$ is the minimum bending stiffness, φ is an angle of twist of beam cross-section in the unstable state, $DD = EI_\omega$ is the warping stiffness, and I_ω is the warping constant. For a common thin-walled beam, assume that the relation B_2/B_1 has a marginal value.

From a theoretical point of view, Eq. (5) describes bending phenomenon in the plane yOz. The deflection in the plane yOz is caused by the unstable state of the beam rather than by bending phenomenon, because B_2/B_1 is negligible.[29] Hence, Eq. (5) is not used for determining deflection v when the beam is in an unstable state. Considering small deformations, beam curvatures in planes xOy and yOz are obtained by the differential equations $d^2u/dz^2 = 1/R_u$ and $d^2v/dz^2 = 1/R_v$ respectively. Beam curvatures in planes xOy and yOz are also correlated by the

formula $R_u = R_v \cdot \varphi$.[26,29,32] From this, a correlated equation in terms of u, v, and φ is as follows:

$$\frac{d^2v}{dz^2} = \frac{d^2u}{dz^2} \cdot \varphi. \tag{8}$$

Substituting internal moments M_η and M_ζ from Eq. (4) into Eqs. (6) and (7), it results in generalized system of differential equations associated with the global coordination *Oxyz* as follows:

$$\varphi \cdot M_x + M_y = B_2 \frac{d^2u}{dz^2}, \tag{9}$$

$$-\left(\frac{d}{dz}u\right) \cdot M_x + M_z = C\frac{d\varphi}{dz} - DD\frac{d^3\varphi}{dz^3}. \tag{10}$$

Thus, Eqs. (8)–(10) are used for defining formulae for deflections u, v, and angle of twist φ, respectively.

Step 5: *Solve the system of differential equations and define deflection and angle of twist.*

In theory, it is possible to solve the system of Eqs. (8)–(10). However, in case of the beam subjected to combined external loads, this system is intricate and so far there have not been a generalized solution based on algebraic methods. Thus, this type of stability problem was frequently solved by using the energy method in accordance with one of the following two approaches.[1,3,26,29]

– *Approach* 1: Here, it has to evalutate an initial approximation of φ satisfying the boundary conditions, and then by using Eqs. (8) and (9) it is possible to determine u and v. This approach is particularly commonly used for the case of simply supported beams due to the fact that M_x and M_y can be easily defined, consequently deflection u is withdrawn from Eq. (9).
– *Approach* 2: First, it is necessary to assess an initial approximation of u satisfying the boundary conditions, and then it is likely to determine φ and v based on Eqs. (8) and (10). Here, it is rather difficult to define φ based on Eq. (10), especially in case $DD = EI_\omega \neq 0$ there will be the third order differential equation with respect to φ. Hence, this approach is conveniently used when dealing with the stability problem of beams with rectangular beam cross-section and $I_\omega = 0$. In this paper, both of these approaches are considered, the results are evaluated one to another for a particular case of rectangular beam cross-section.

Step 6: *Determination of expressions describing critical state of the system based on energy method*

On the basis of the formulae of u, v and φ, it needs to formulate the elastic strain energy of the beam and work caused by external loads. In this work, a novel approach to define work caused by external loads is suggested. As a matter of fact, in a

conservative system, work caused by combined bending loads can be defined by work of internal moment. This in fact makes the calculation process much simpler.[5] Therefore, the critical state of the system is described by the extremum condition of the total energy.[29]

Based on the abovementioend procedure, two cases are considered. The first one was a thin-walled beam subjected to axial force F, bending moment M, and concentrated load P. For the second, load P was replaced by a uniform partially distributed load q.

1. Case 1 — Beam under combined loads M-P-F

The beam is subjected simultaneously to moment M, force F, and load P at beam center, as shown in Fig. 1. Bearing in mind a general context, load P application point is located at height c in relation to gravity center of the beam cross-section. Here, an angle of twist φ is estimated approximately according to boundary conditions of a simply supported beam, as presented in the next equation:

$$\varphi = \varphi_0 \cos\left(\frac{\pi \cdot z}{L}\right), \tag{11}$$

where φ_0 is a constant. Based on Eq. (9), deflection $u$can be defined. If so, it is necessary to determine internal moments M_x and M_y as follows.

Internal moment M_x:

$$M_x = M + \frac{P}{2}\left(\frac{L}{2} - z\right). \tag{12}$$

Internal moment M_y:

$$M_y = -F \cdot u. \tag{13}$$

By using Eqs. (9), (12), (13) and boundary condition causing $u(L/2) = 0$ and $du/dz(L/2) = 0$, deflection u is as follows:

$$\begin{aligned} u = {} & \cos\left(\frac{\sqrt{F}z}{\sqrt{B_2}}\right)m_1 + \sin\left(\frac{\sqrt{F}z}{\sqrt{B_2}}\right)m_2 \\ & + \frac{1}{4}\frac{L^2}{H^2}\left[-(LP - 2Pz + 4M)H\cos\left(\frac{\pi z}{L}\right) - 4B_2 L \sin\left(\frac{\pi z}{L}\right)\pi P\right], \end{aligned} \tag{14}$$

where m_1 and m_2 are constants, which can be found based on the boundary condition when dealing with the differential Eq. (9), and they are provided in detail in Appendix A. To simplify the formula, several additional parameters are used such as: $H = B_2\pi^2 - FL^2; k = L\sqrt{F}/2\sqrt{B_2}$. Moreover, elastic strain energy of the beam can be derived from the following expression[1–3]:

$$U = B_2 \int_0^{\frac{L}{2}} \left(\frac{d^2u}{dz^2}\right)^2 \cdot dz + C \int_0^{\frac{L}{2}} \left(\frac{d\varphi}{dz}\right)^2 \cdot dz + DD \int_0^{\frac{L}{2}} \left(\frac{d^2\varphi}{dz^2}\right)^2 \cdot dz. \tag{15}$$

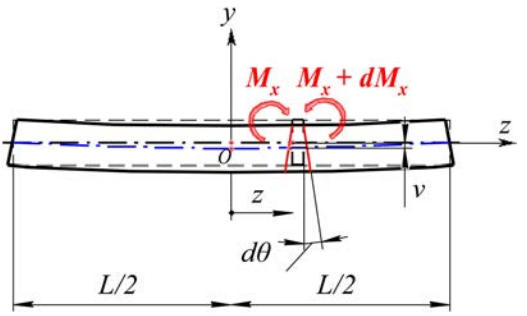

Fig. 3. Determination of work caused by internal force in detail.

In order to define work caused by external loads, generally the initial stage is to find deflection v from Eq. (8). Nevertheless, for the beam subjected to combined external loads, the obtained expression of v is very complicated.[1,26,29] Considerding $d\theta$ to be an angle of twist of cross-section element dz, illustrated in Fig. 3, it turns out:

$$dW_{MP} = M_x d\theta = M_x v'' dz. \tag{16}$$

According to Eq. (8), there is $v'' = u'' \cdot \varphi$, it yields:

$$dW_{MP} = M_x v'' dz = M_x u'' \varphi dz. \tag{17}$$

Here, work W_{MP} caused by combined loads M and P is:

$$W_{MP} = 2\int_0^{\frac{L}{2}} dW_{MP} = 2\int_0^{\frac{L}{2}} (M_x u''\varphi) \cdot dz. \tag{18}$$

It is noteworthy that force F does not cause v and θ of beam cross-section in the plane xOz, but it results in horizontal deflection u in the plane yOz. Thus, work caused by axial force F can be defined by the following expression[1,29]:

$$W_F = F\int_0^{\frac{L}{2}} \left(\frac{du}{dz}\right)^2 \cdot dz. \tag{19}$$

Since there is a distance c between load P application point and gravity center of cross-section, as the beam is deformed, there exists an additional displacement of application point as follows (Fig. 1):

$$c(1 - \cos\varphi(0)) = c\left(2\sin^2\frac{\varphi(0)}{2}\right) \approx \frac{c[\varphi(0)]^2}{2}. \tag{20}$$

For that reason, the additional work caused by concentrated load P is as follows[1]:

$$W_d = \frac{1}{2} \cdot P \cdot c \cdot [\varphi(0)]^2. \tag{21}$$

The overall work caused by external loads W:

$$W = W_{MP} + W_F + W_d. \tag{22}$$

Substituting Eqs. (18), (19), (21) into Eq. (22), it results in:

$$W = 2\int_0^{\frac{L}{2}} (M_x u''\varphi)\cdot dz + \frac{1}{2}\cdot P\cdot c\cdot [\varphi(0)]^2 + F\int_0^{\frac{L}{2}} \left(\frac{du}{dz}\right)^2 \cdot dz. \tag{23}$$

As long as the critical state of the system is described by the extremum condition of the total energy[1,3,26,29]:

$$\delta(U - W) = 0. \tag{24}$$

Substituting the expressions of U and W into Eq. (24), the algebraic equation describing the critical state of the beam is obtained as follows:

$$\begin{aligned} RP = {} & \sqrt{B_2}H(\cos(k))^2[-24B_2FL^7\pi^2P(-M\pi^2 + LP) \\ & - 2L^6P^2(-B_2FL^2\pi^4 + 3B_2^2\pi^4 + 9F^2L^4) \\ & - L^5\pi^2P(B_2^2\pi^4 + F^2L^4)(LP + 12M) - 48L^4MH^2(M\pi^2 + LP) \\ & + 48H^3(CL^2\pi^2 + DD\pi^4 - 2L^3Pc)] - 96B_2^2F^{3/2}L^9\pi^2P^2\sin(2k) \\ & + 12B_2L^7\sqrt{F}P^2(B_2{\pi^2} + FL^2)^2\sin(4k) \\ & - 96FL^8\pi B_2^{3/2}P^2(B_2\pi^2 + FL^2)\cos(k)\cos(2k) \\ & + 288FL^8\pi B_2^{3/2}P^2(B_2\pi^2 + FL^2)\cos(k) \\ & - 96FL^8\pi B_2^{3/2}P^2(B_2\pi^2 + FL^2)\sin(k)\sin(2k) \\ & - 48B_2L^7\sqrt{F}P^2(B_2{\pi^2} + FL^2)^2\sin(2k)(\cos(k))^2 = 0. \end{aligned} \tag{25}$$

Based on the generalized expression (25), several individual scenarios are analyzed such as:

When $c = 0$, from Eq. (25) there is:

$$\begin{aligned} & \sqrt{B_2}H^2\cdot[48L^7\sqrt{B_2F}P^2(B_2^2\pi^4 + 6B_2FL^2\pi^2 + F^2L^4)\sin(k) \\ & - 192FL^8\pi B_2P^2(B_2\pi^2 + FL^2) + H\cos(k)\cdot(12L^4M(B_2^2\pi^4 + F^2L^4) \\ & \times (LP\pi^2 + 4M\pi^2 + 4LP) - 48\pi^2H^3(CL^2 + DD\pi^2) \\ & - 96B_2FL^6M\pi^2(M\pi^2 + LP) + 24B_2FL^7\pi^2P(-M\pi^2 + LP) \\ & + F^2L^{10}P^2(\pi^2 + 18) + B_2^2L^6\pi^4P^2(\pi^2 + 6) - 2B_2FL^8P^2\pi^4)] = 0. \end{aligned} \tag{26}$$

When $c = 0$ and $DD = 0$ (rectangular cross-section), Eq. (25) can be simplified:

$$\begin{aligned} & \sqrt{B_2}H^2\cdot[48L^7\sqrt{B_2F}P^2(B_2^2\pi^4 + 6B_2FL^2\pi^2 + F^2L^4)\sin(k) \\ & - 192FL^8\pi B_2P^2(B_2\pi^2 + FL^2) + H\cos(k)\cdot(12L^4M(B_2^2\pi^4 + F^2L^4) \\ & \times (LP\pi^2 + 4M\pi^2 + 4LP) - 48\pi^2H^3CL^2 - 96B_2FL^6M\pi^2(M\pi^2 + LP) \\ & + 24B_2FL^7\pi^2P(-M\pi^2 + LP) + F^2L^{10}P^2(\pi^2 + 18) \\ & + B_2^2L^6\pi^4P^2(\pi^2 + 6) - 2B_2FL^8P^2\pi^4)] = 0. \end{aligned} \tag{27}$$

When $F = 0$ and $P = 0$, from Eq. (25) the critical moment M_{cr} is:

$$M_{cr} = \frac{\pi\sqrt{B_2(CL^2 + DD\pi^2)}}{L^2}. \tag{28}$$

When $M = 0$ and $P = 0$, from Eq. (25) the critical axial force F_{cr} is:

$$F_{cr} = \frac{\pi^2 B_2}{L^2}. \tag{29}$$

And when $M = 0$ and $F = 0$, from Eq. (25) the critical load P_{cr} is:

$$P_{cr} = \frac{4\sqrt{3(\pi^2+6)}\pi^2\sqrt{B_2(CL^2 + DD\pi^2)}}{(\pi^2+6)L^3} = \frac{17.16\sqrt{B_2(CL^2 + DD\pi^2)}}{L^3}. \tag{30}$$

The obtained critical load P_{cr} for the individual cases in accordance with Eqs. (28) and (29) complies with the results yielded from the exact solution, which can be found in the work of several authors.[1–5] According to these references, the critical load obtained from the exact solution of differential equations is: $P_{cr} = 16.94\sqrt{B_2 C}/L^2$, hence the deviation of coefficient with respect to that of Eq. (30) is insignificant only 1.3% (16.94 versus 17.16).

With the aim to illustrate the stability region boundary of the beam in a graphical form, as an example, a thin-walled I-profile beam has the following parameters: $E = 2.07 \cdot 10^{11}$ Pa; $\mu = 0.28$; $\rho = 7800\,\mathrm{kg/m^3}$, and beam geometry is as follows: $L = 3$ m; $h = 0.1$ m; $b = 0.04$ m; $t_1 = t_2 = 0.004$ m. In case, the beam is subjected to an individual loading (M, F, or P), the critical values are: $M_{cr} = 1801.3$ N m, $F_{cr} = 9796.7$ N, $P_{cr} = 3290.1$ N (with $c = 0$).

The boundary surface of the stability region RP (Eq. (25)) of the beam in the space of M-F-P at different values of c can be observed in Fig. 4. The graph indicates that once c increases, P_{cr} decreases or the beam might turn to be unstable and vice versa. This observation is in aggrement with the theory of thin-walled beams.[1,2] The obtained property of the stability region boundary also complies with Papkovitch's theorem.[25,29]

2. Case 2 — Beam under combined loads M-q-F

Here, the beam is subjected to force F, moment M, and partially distributed load q over the length of αL, as shown Fig. 5, in which α is a dimensionless coefficient: $0 \leq \alpha \leq 1$. It is noted that this case is much more complicated in comparison with the previous one, and yet it is also a representative sample for the case of load q over the full beam length or of load P at beam center. For this case, two important approaches are used for dealing with the concerned problem, as mentioned before.

2.1. *Estimate φ prior to determination of u*

This first approach presents a calculation procedure similar to the previous case. The angle of twist φ is also estimated in accordance with the boundary condition of the beam based on Eq. (11). From Eq. (9), in order to find the deflection u, it needs to

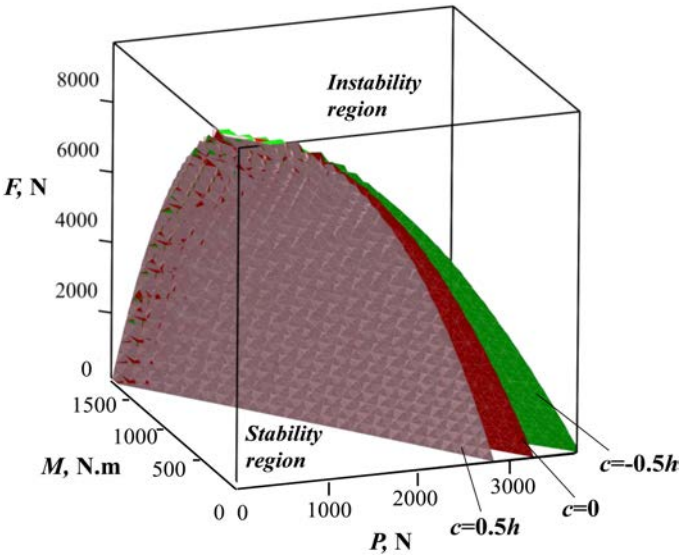

Fig. 4. Stability region boundary surfaces of I-profile beam in the space of M-F-P at different values of c.

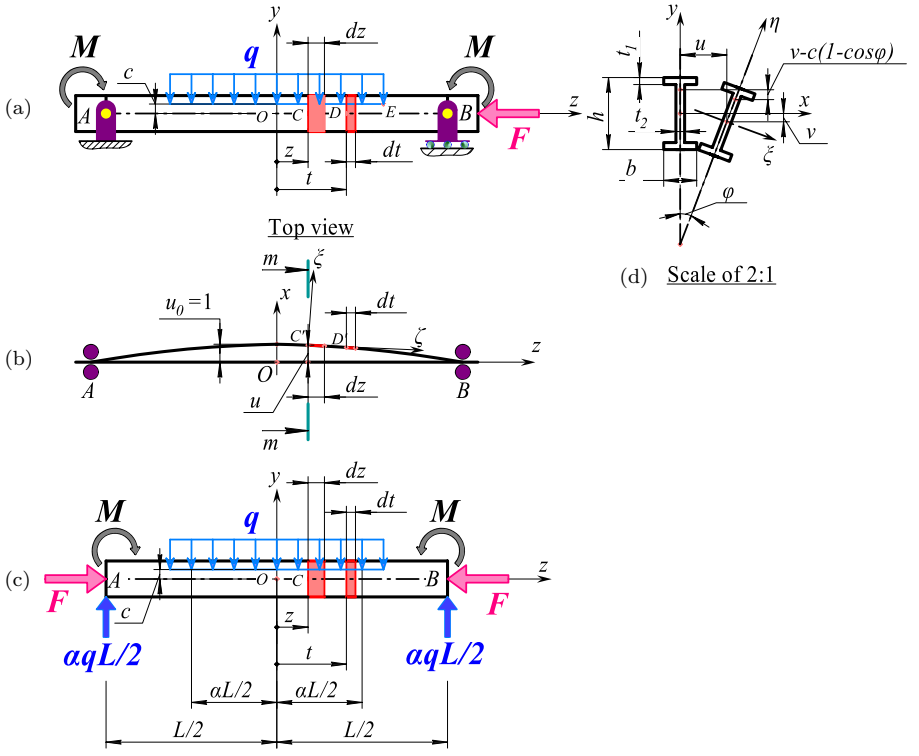

Fig. 5. Scheme of the beam under combined loads M-q-F.

determine M_x and M_y. The load q is only located on the segment OE, but not on the EB (Fig. 5). This makes the calculation much more challenging in comparison with the case of uniform distributed load q over the full beam length, which was studied by the authors,[29] because herein M_x and M_y on the segments OE and EB are defined by different formulas.

On the segment OE, bending moment M_{x1} can be defined as follows:

$$M_{x1} = M + \alpha \cdot q \cdot \frac{L}{2}\left(\frac{L}{2} - z\right) - \frac{1}{2}q\left(\alpha \cdot q \cdot \frac{L}{2} - z\right)^2. \tag{31}$$

And on the segment EB, bending moment M_{x2} is:

$$M_{x2} = M + \alpha \cdot q \cdot \frac{L}{2}\left(\frac{L}{2} - z\right). \tag{32}$$

Bending moment M_{y1} on the segment OE is:

$$M_{y1} = -F \cdot u_1. \tag{33}$$

Also, bending moment M_{y2} on the segment EB is:

$$M_{y2} = -F \cdot u_2. \tag{34}$$

Besides, formulas of u_1 and u_2 corresponding to the deflections on the segments OE and EB, respectively, need to be in accordance with the boundary condition and principle of continuity:

$$u_1\left(\frac{L}{2}\right) = 0, \quad u_1\left(\frac{\alpha L}{2}\right) = u_2\left(\frac{\alpha L}{2}\right), \quad \frac{du_1}{dz}\left(\frac{\alpha L}{2}\right) = \frac{du_2}{dz}\left(\frac{\alpha L}{2}\right) \quad \text{and} \quad \frac{du_1}{dz}(0) = 0.$$

Substituting Eqs. (31)–(34) into Eq. (9), the expressions for u_1 and u_2 are as follows:

$$u_1 = \varphi_0\left\{u_{11}\cos\left(\frac{\pi z}{L}\right)z^2 + u_{12}\sin\left(\frac{\pi z}{L}\right)z + \sin\left(\frac{\sqrt{F}z}{\sqrt{B_2}}\right)c_2 + \cos\left(\frac{\sqrt{F}z}{\sqrt{B_2}}\right)c_1 + u_{13}\cos\left(\frac{\pi z}{L}\right)\right\} \tag{35}$$

and

$$u_2 = \varphi_0\left\{u_{21}\cos\left(\frac{\pi z}{L}\right)z + \sin\left(\frac{\sqrt{F}z}{\sqrt{B_2}}\right)c_4 + \cos\left(\frac{\sqrt{F}z}{\sqrt{B_2}}\right)c_3 + u_{22}\cos\left(\frac{\pi z}{2L}\right) + u_{23}\sin\left(\frac{\pi z}{2L}\right)\right\}, \tag{36}$$

where u_{11}, u_{12}, u_{13}, u_{21},u_{22}, u_{23} — parameters independent from z — and constants c_1, c_2, c_3, c_4, which can be determined based on the boundary condition of u_1 and u_2 are given in Appendix A.

In this case, elastic strain potential energy of the beam is obtained from the following expression[1–3]:

$$U = B_2 \int_0^{\alpha\frac{L}{2}} \left(\frac{d^2u_1}{dz^2}\right)^2 dz + B_2 \int_{\alpha\frac{L}{2}}^{\frac{L}{2}} \left(\frac{d^2u_2}{dz^2}\right)^2 dz + C \int_0^{\frac{L}{2}} \left(\frac{d\varphi}{dz}\right)^2 dz + DD \int_0^{\frac{L}{2}} \left(\frac{d^2\varphi}{dz^2}\right)^2 dz. \tag{37}$$

In the similar way as explained above, the work W_{Mq} caused by external combined loads M and q can be defined through work of internal forces as follows:

$$W_{Mq} = 2\int_0^{\frac{L}{2}} dW_{Mq} = 2\int_0^{\alpha\frac{L}{2}} (M_{x1}u_1''\varphi)\cdot dz + 2\int_{\alpha\frac{L}{2}}^{\frac{L}{2}} (M_{x2}u_2''\varphi)\cdot dz. \tag{38}$$

The work caused by axial force F is defined similarly according to Eq. (19), but here it needs to determine for two segments OE and EB separately:

$$W_F = F\int_0^{\alpha\frac{L}{2}} \left(\frac{du_1}{dz}\right)^2 dz + F\int_{\alpha\frac{L}{2}}^{\frac{L}{2}} \left(\frac{du_2}{dz}\right)^2 dz. \tag{39}$$

The additional work, due to the fact that application line of uniform distributed load q does not coincide with the central line of the beam, similarly as stated in previous section, is:

$$W_d = 2\int_0^{\alpha\frac{L}{2}} qc(1-\cos\varphi)\cdot dz = 2\int_0^{\alpha\frac{L}{2}} q\frac{c\varphi^2}{2}\cdot dz. \tag{40}$$

The overall work W caused by external loads is defined by Eq. (22). Substituting Eqs. (38)–(40) into Eq. (22), it results in:

$$W = 2\int_0^{\alpha\frac{L}{2}} \left(M_{x1}\cdot\frac{d^2u_1}{d^2z}\cdot\varphi\right)dz + 2\int_{\alpha\frac{L}{2}}^{\frac{L}{2}} \left(M_{x2}\cdot\frac{d^2u_2}{d^2z}\cdot\varphi\right)dz + 2\int_0^{\alpha\frac{L}{2}} \left(q\frac{c}{2}\varphi^2\right)dz + F\int_0^{\alpha\frac{L}{2}} \left(\frac{du_1}{dz}\right)^2 dz + F\int_{\alpha\frac{L}{2}}^{\frac{L}{2}} \left(\frac{du_2}{dz}\right)^2 dz. \tag{41}$$

Yet, the critical state of the system is described by the extremum condition of the total energy according to Eq. (24). Substituting the formulas of U and W into Eq. (24), there will be an algebraic equation describing the critical state of the beam as follows:

$$R = R_1 + R_2 + R_3 + R_4 + R_5 + R_6 + R_7 + R_8 = 0, \tag{42}$$

where R_i are supplemental expressions and given in Appendix A.

The generalized expression $R = 0$ describes stability region boundary of the beam under force F, moment M, and load q. Several individual scenarios are evaluated:

From Eq. (42), the critical moment M_{cr} is obtained for the case $F = 0$ and $q = 0$ in accordance with Eq. (28).

From Eq. (42), the critical axial force F_{cr} is obtained for the case $M = 0$ and $q = 0$ in accordance with Eq. (29).

Based on Eq. (42), the critical uniform distributed load q_{cr} is obtained for the case $M = 0$, $F = 0$, $c = 0$ and $\alpha = 1$ as follows:

$$q_{\text{cr}} = \frac{2\sqrt{30}\pi^3\sqrt{(\pi^4+45)B_2(CL^2+DD\pi^2)}}{(\pi^4+45)L^4} = \frac{28.46\sqrt{B_2(CL^2+\pi^2DD)}}{L^4} \tag{43}$$

According to several researchers,[1,2] the load q_{cr}, which is obtained from the exact differential solution, is $q_{\text{cr}} = 28.30\sqrt{B_2C}/L^3$, thus the deviation of coefficient with respect to that of (43) is only 0.56% (28.30 versus 28.46).

When $c = 0$ and $\alpha = 1$, from Eq. (42) there is a following equation:

$$\begin{aligned}
&-2B_2^2F^2L^4\pi^4[-360L^4M^2\pi^4 + 600B_2CL^2\pi^6 + 600B_2DD\pi^8 - 60L^6M\pi^2(3+\pi^2)q \\
&\quad + L^8(795 + 25\pi^2 - 3\pi^4)q^2] + 2B_2F^3L^6\pi^2[-240L^4M^2\pi^4 + 600B_2CL^2\pi^6 \\
&\quad + 600B_2DD\pi^8 - 40L^6M\pi^2(3+\pi^2)q + L^8(60 + 5\pi^2 - 2\pi^4)q^2] \\
&\quad + 2B_2^3FL^2\pi^6[-240L^4M^2\pi^4 + 300B_2CL^2\pi^6 + 300B_2DD\pi^8 \\
&\quad - 40L^6M\pi^2(3+\pi^2)q + L^8(-240 + 15\pi^2 - 2\pi^4)q^2] - B_2^4\pi^8[-120L^4M^2\pi^4 \\
&\quad + 120B_2CL^2\pi^6 + 120B_2DD\pi^8 - 20L^6M\pi^2(3+\pi^2)q - L^8(45+\pi^4)q^2] \\
&\quad + F^4L^8[120L^4M^2\pi^4 - 600B_2CL^2\pi^6 - 600B_2DD\pi^8 + 20L^6M\pi^2(3+\pi^2)q \\
&\quad + L^8(-15 + 10\pi^2 + \pi^4)q^2] + 120F^5L^{10}\pi^4(CL^2 + DD\pi^2) \\
&\quad + 480B_2^{3/2}F^{3/2}L^{11}\pi^4Hq^2\tan k = 0.
\end{aligned} \tag{44}$$

When $c = 0$, $\alpha = 1$ and $DD = 0$, from Eq. (42), there is an expression describing the stability region of the beam with rectangular cross-section as follows:

$$\begin{aligned}
&-120C\pi^4H^5 + B_2^4\pi^8L^2(120M^2\pi^4 + 20L^2M\pi^2(3+\pi^2)q + L^4(45+\pi^4)q^2) \\
&\quad + F^4L^{10}(120M^2\pi^4 + 20L^2M\pi^2(3+\pi^2)q + L^4(-15 + 10\pi^2 + \pi^4)q^2) \\
&\quad - 2B_2^3FL^4\pi^6(240M^2\pi^4 + 40L^2M\pi^2(3+\pi^2)q + L^4(240 - 15\pi^2 + 2\pi^4)q^2) \\
&\quad - 2B_2F^3L^8\pi^2(240M^2\pi^4 + 40L^2M\pi^2(3+\pi^2)q + L^4(-60 - 5\pi^2 + 2\pi^4)q^2) \\
&\quad + 2B_2^2F^2L^6\pi^4(360M^2\pi^4 + 60L^2M\pi^2(3+\pi^2)q + L^4(-795 - 25\pi^2 + 3\pi^4)q^2) \\
&\quad + 480B_2^{3/2}F^{3/2}L^9\pi^4Hq^2\tan k = 0.
\end{aligned} \tag{45}$$

Equations (44) and (45) coincide with the results obtained by the author in the previous work.[29] It is important to note that when $\alpha \to 0$, from Eq. (42) it is possible to derive the expression $RP = 0$, which describes the stability region boundary of the beam under force F, moment M, and load P at beam center, similar to Eq. (25) in the first case. The expression RP is defined by substituting $q = P/\alpha L$ into Eq. (42)

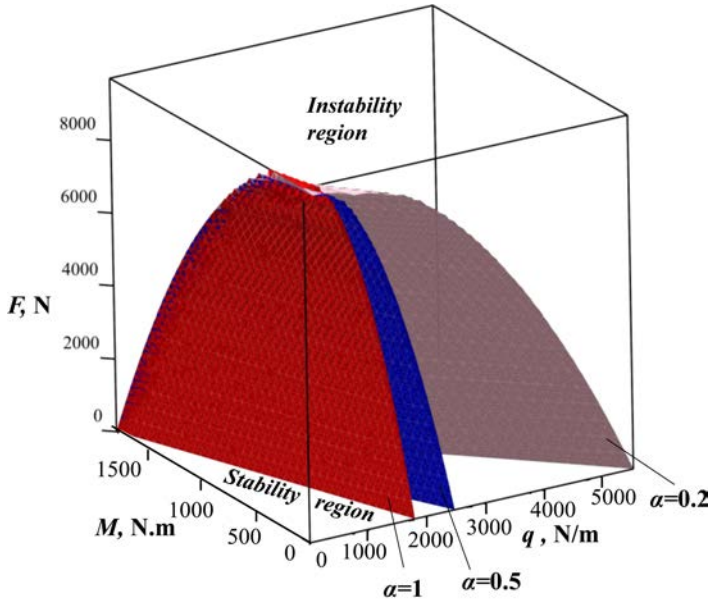

Fig. 6. Stability region boundary surfaces of I-profile beam in the space of M-F-q when c=0 and at different values of α.

and then using the following formula:

$$RP = \lim_{\alpha \to 0} R. \tag{46}$$

As a result, this second case is a generalized form of the first one and of the case in which the load q is applied over the full beam length, as analyzed before by the authors.[29] In order to represent the stability region boundary of beam visually in graphical form, the same thin-walled I-profile beam is considered. For the cases of an individual loading (M, F, or q), the corresponding critical results are: $M_{\rm cr} = 1801.3\,{\rm N\,m}$, $F_{\rm cr} = 9796.7\,{\rm N}$, $q_{\rm cr} = 1813.3\,{\rm N/m}$ (with $c = 0$).

The stability region boundary surface R of the beam in the space of M, F, q at different values of α can be observed in Fig. 6. The graph indicates that once α decreases, i.e. effect length of uniform distributed load q reduces, the critical value $q_{\rm cr}$ increases crucially. Meanwhile, the boundary surfaces of different c values and the case of fully distributed load q or $\alpha = 1$ can be seen in Fig. 7. It indicates that once c increases, $q_{\rm cr}$ decreases or the beam might turn to be unstable and vice versa.

2.2. *Estimate u prior to determination of φ*

This second approach to dealing with the problem is that first it is necessary to estimate deflection u in accordance with the boundary condition, and then to define angle of twist φ based on Eq. (10). Doing so, Eq. (10) turns to be the third order differential equation with respect to φ, hence the outcomes would be cumbersome

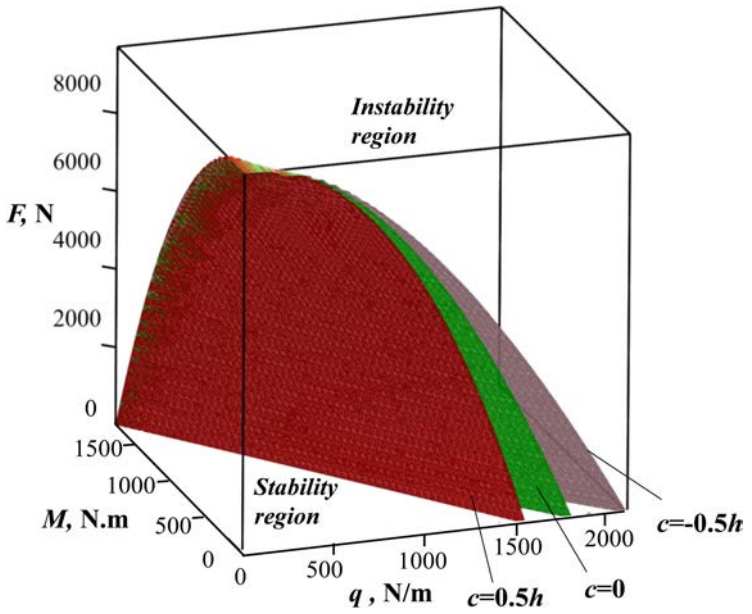

Fig. 7. Stability region boundary surfaces of I-profile beam in the space of M-F-q when $\alpha = 1$ and at different values of c.

and complex. Thus, in order to represent the second approach, the beam with a rectangular cross-section ($DD = 0$) is considered for convenience, while other conditions are kept the same as decribed before in previous section (Fig. 5).

In order to comply with the boundary condition, u is estimated approximately as follows:

$$u = u_0 \cos\left(\frac{\pi \cdot x}{L}\right). \tag{47}$$

By the similar problem-solving approach, the expression for φ is defined according to Eq. (10) at the segments OE and EB such as:

On the OE:

$$\begin{aligned}\varphi_1 = \frac{1}{8C\pi^2}\Big\{&q\alpha^2 L^2 \cos\left(\frac{\pi z}{L}\right)\pi^2 - 2\alpha q L^2 \cos\left(\frac{\pi z}{L}\right)\pi^2 + 4L^2\pi \sin\left(\frac{\alpha\pi}{2}\right)\alpha q \\ &+ 4\pi^2 \cos\left(\frac{\pi z}{L}\right)qz^2 - 4L^2\pi \sin\left(\frac{\alpha\pi}{2}\right)q + 8L^2\pi\alpha q - 16L\pi \sin\left(\frac{\pi z}{L}\right)qz \\ &- 24L^2 \cos\left(\frac{\pi z}{L}\right)q + 24L^2 \cos\left(\frac{\alpha\pi}{2}\right)q - 8M \cos\left(\frac{\pi z}{L}\right)\pi^2\Big\}.\end{aligned} \tag{48}$$

And on the EB:

$$\begin{aligned}\varphi_2 = -\frac{1}{4C\pi}\Big\{&\alpha q L^2 \cos\left(\frac{\pi z}{L}\right)\pi - 2L\pi \cos\left(\frac{\pi z}{L}\right)\alpha qz + 4\alpha q L^2 \sin\left(\frac{\pi z}{L}\right) \\ &+ 2q \sin\left(\frac{\alpha\pi}{2}\right)L^2 - 4\alpha q L^2 - 4q \sin\left(\frac{\alpha\pi}{2}\right)Lz + 4M \cos\left(\frac{\pi z}{L}\right)\pi\Big\}.\end{aligned} \tag{49}$$

The expression describing the boundary surface of the stability region derived from Eq. (24) is:

$$S = S_1 cq^3 + S_2 cMq^2 + S_3 q^2 + S_4 cM^2 q + S_5 Mq + S_6 M^2 + S_7 F + S_8 = 0, \quad (50)$$

where S_i are constants, which are independent from M, q, F, c and details are given in Appendix A.

When $M = 0$ and $q = 0$, from Eq. (50) it is possible to derive the critical axial force F_{cr} as same as Eq. (29).

When $F = 0$ and $q = 0$, from Eq. (50) the critical moment M_{cr} is:

$$M_{\text{cr}} = \frac{\pi\sqrt{B_2 C}}{L} \quad (51)$$

When $M = 0$, $F = 0$ and $\alpha = 1$, from Eq. (50), the crititial uniform distributed load q_{cr} is:

$$q_{\text{cr}} = \frac{28.86\sqrt{B_2 C}}{L^3}. \quad (52)$$

Formula (51) is equivalent to the previous one (28) when $DD = 0$, and it is also in agreement with the result in the previous work.[29] The deviation of coefficient between the one of (52) and the aforementioned one from the exact differential solution is only 1.98% (28.30 versus 28.86).[1,2] It could be neglected in practical engineering applications. Hence, it is evident that the deviation of coefficient from this second approach is greater than that from the first approach.

From Eq. (50), when $c = 0$, it is possible to obtain the expression describing the stability region of the beam under moment M, force F and partially distribute load q as follows:

$$\begin{aligned} &-240CL^2M^2\pi^7 - 20ML^4C\pi^4 q(6\sin(\alpha\pi) - \pi^3\alpha^3 + 3\pi(\pi^2+2)\alpha) - L^6C\pi^2q^2 \\ &\quad \times \left(30(-\pi^2\alpha^2 + \pi^2\alpha - 33)\sin(\alpha\pi) + 30\pi(\alpha-8)\cos(\alpha\pi) - 1920\alpha\pi\sin\left(\frac{\alpha\pi}{2}\right)\right) \\ &\quad + L^6C\pi^2q^2(2\pi^5\alpha^5 - 5\pi^5\alpha^4 - 120\pi^3\alpha^3 + 5\pi^3\alpha^2(\pi^2+36) + 960\alpha\pi + 240\pi) \\ &\quad - 240F\pi^7L^2C^2 + 240B_2\pi^9C^2 = 0. \end{aligned} \quad (53)$$

From Eq. (50), when set $c = 0$ and $\alpha = 1$, the expression describing the stability region of the beam under M, F and fully distributed load q is:

$$\begin{aligned} &-240CL^2M^2\pi^7 + (-40CL^4\pi^7 - 120CL^4\pi^5)qM + (-2CL^6\pi^7 - 60CL^6\pi^5 \\ &\quad + 510CL^6\pi^3)q^2 + 240B_2\pi^9C^2 - 240F\pi^7L^2C^2 = 0. \end{aligned} \quad (54)$$

When $\alpha \to 0$, similarly from Eq. (50), it is possible to derive the expression describing the stability region of the beam under M, F and load P at beam center. If $c = 0$, the resultant equation is:

$$\begin{aligned} &-5CL^4P^2\pi^7 - 60CL^3MP\pi^7 + 240B_2\pi^9C^2 - 240F\pi^7L^2C^2 - 330CL^4P^2\pi^5 \\ &\quad - 240CL^2M^2\pi^7 + 960CL^4P^2\pi^4 - 240CL^3MP\pi^5 = 0. \end{aligned} \quad (55)$$

Comparing Eqs. (54) with (45) and (55) with (27), it is noted that the recently obtained expressions from the second approach are more convenient and user-friendly than the first one in practice.

3. Evaluation of the Results

It is important to note that in the case of thin-walled beams subjected to individual loading, the critical values can be derived accurately by solving the system of differential equations. In fact, they could also be obtained according to the expressions (28)–(30), (43), (51), (52); besides they are also in agreement with those obtained from the exact solutions, which were presented before in several works.[1–5,29] An accuracy of the expression (44) for an I-profile beam was verified by FEM-based NX Nastran® software in the recent publication.[17,29] The outcome pointed out that the expression was reliable and feasible to use in practical calculation.

3.1. *Accuracy of the expressions for a rectangular beam cross-section*

This section is dedicated to the analysis of an accuracy of the generalized expression (42) from the first approach and of the expression (50) from the second approach especially for the case of rectangular cross-section thin-walled beam ($DD = 0$) subjected to combined external loads. The load q is located at the central area of the beam, and effect length is a half of beam length, i.e. $\alpha = 0.5$, and load q application line coincides with the central line of the beam, i.e. $c = 0$. Yet, in this paper, the accuracy analysis of the system is verified by means of the FEM-based ANSYS® software.[15,16]

Considering that a thin-walled beam has the following parameters: $E = 2.07 \cdot 10^{11}\,\text{Pa}$; $\mu = 0.28$; $\rho = 7800\,\text{kg/m}^3$, and geometry: length $L = 0.8\,\text{m}$; height $h = 0.08\,\text{m}$; breadth $b = 0.004\,\text{m}$. In case of individual loading, the critical values according to Eq. (42) are as follows: $M_{\text{cr}} = 433.5\,\text{N m}$, $F_{\text{cr}} = 1362.0\,\text{N}$, $q_{\text{cr}} = 8658.0\,\text{N/m}$.

The graphs describing the boundary of stability region on surfaces *M-q, M-F*, and *q-F* according to (42) and (50) do not show any differences among them, as it can be observed in Figs. 8–10.

As a matter of fact by using the software, it is truly hard to analyze and illustrate the boundary of stability region similar to that shown in Figs. 4 and 6–10. These softwares merely allow for verification of the beam state based on stability safety factor (n_{stab}) for a determined individual load (M, q, F). Regarding the points inside of the stability region, the safety factor derived from the software would be greater than 1 ($n_{\text{stab}} > 1$), while for the points outside of the stability region, the factor would be smaller than 1 ($n_{\text{stab}} < 1$), and with respect to the points right on the stability region boundary this factor is unity ($n_{\text{stab}} = 1$). Hence, test method is carried out as follows.

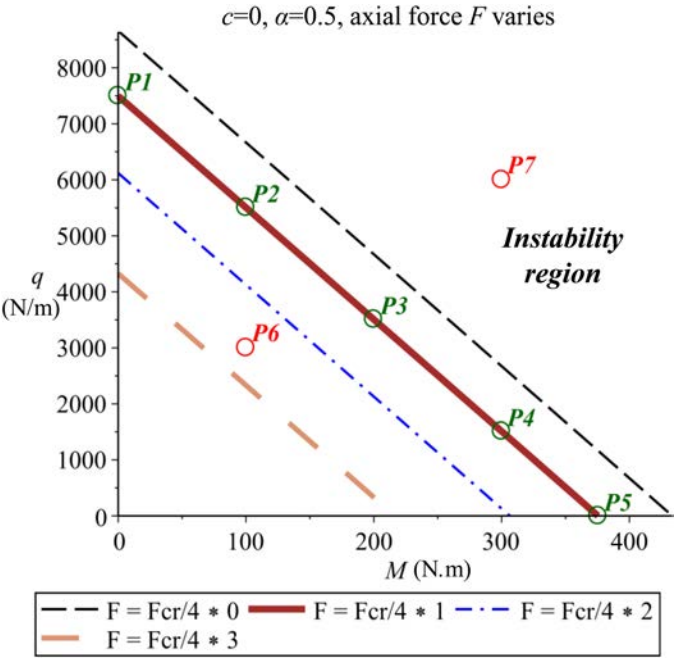

Fig. 8. Boundary of stability region of a rectangular cross-section thin-walled beam with variation of axial force F.

Using the expressions (42) and (50) (corresponding to $\alpha = 0.5$, $c = 0$), it is possible to select five sets of parameters (M, q, F) being on the border of the stability region (points P_1–P_5 on the curve $F = F_{cr}/4$, Fig. 8). Besides, a single set (M, q, F) inside of the stability region (beneath the curve $F = F_{cr}/4$ there is P_6) and another single set outside of the stability region (above the curve $F = F_{cr}/4$ there is P_7) were obtained. These predefined seven sets of parameter (M, q, F) are established as input data for computational program in order to find stability safety factor for the concerned beam. The obtained results, as given in Table 1, indicate that the first five sets (P_1–P_5) being on the border of the stability region yield safety factor $n_{stab} \approx 1$, for the point being inside of the stability region P_6 there is $n_{stab} > 1$ and consequently $n_{stab} < 1$ for the one being outside of the stability region P_7 (Fig. 8).

Similarly, seven sets of parameters (M, q, F) each on Figs. 9 and 10 are selected corresponding to the points P_8–P_{21} (Table 1). The outcomes are obtained such as 10 sets being on the border of stability region (P_8–P_{12} and P_{15}–P_{19}) with safety factor $n_{stab} \approx 1$, whereas two sets being inside of the stability region (P_{13} and P_{20}) with $n_{stab} > 1$ and another two sets being outside of the stability region (P_{14}–P_{21}) with $n_{stab} < 1$.

Therefore, all of 21 test points demonstrate expected results and this also proves the correctness and accuracy of generalized expressions (42) and (50), which are derived by two different approaches. Moreover, numerical analysis shows that

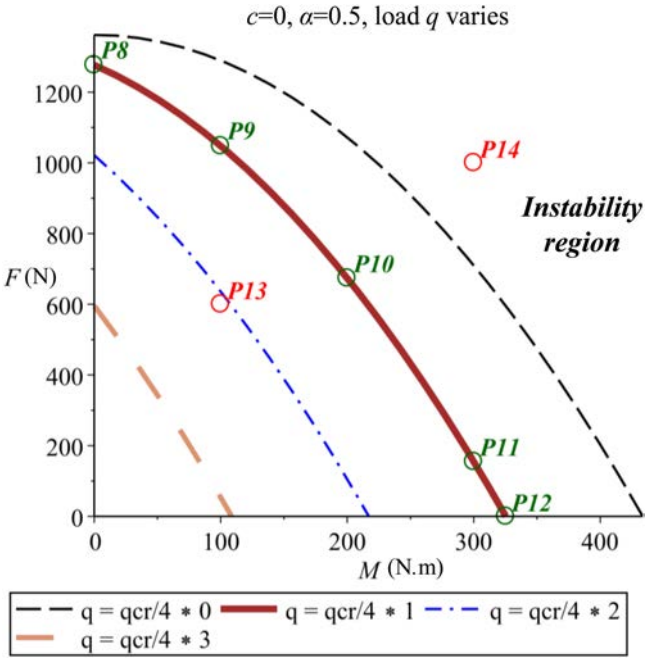

Fig. 9. Boundary of stability region of a rectangular cross-section thin-walled beam with variation of uniform distributed load q.

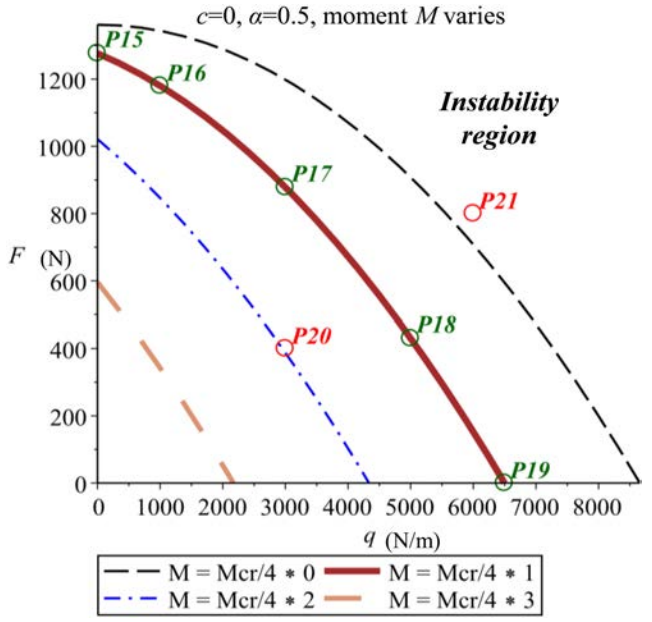

Fig. 10. Boundary of stability region of a rectangular cross-section thin-walled beam with variation of moment M.

Table 1. Stability safety factor of a rectangular cross-section thin-walled beam under combined external loads.

		Parameter set (M, q, F) obtained from the expression (42) or from the graph (φ prior to u — Sec. 4.1)			Parameter set (M, q, F) obtained from the expression (50) or from the graph (u prior to φ — Sec. 4.2)				Ansys (φ prior to u)	Ansys (u prior to φ)
	Test points	M[N.m]	q[N/m]	F[N]	M[N.m]	q[N/m]	F[N]	Point location	BLF value — n_{stab}	
P_1	Fig. 8, location with	0	7374.5	**340.5**	0	7498.0	**340.5**	On the border	0.99	0.97
P_2	respect to the curve	100	5438.2	**340.5**	100	5505.1	**340.5**	On the border	0.99	0.98
P_3	$F = F_{\text{cr}}/4 * 1$	200	3481.8	**340.5**	200	3509.2	**340.5**	On the border	0.99	0.99
P_4		300	1505.1	**340.5**	300	1510.3	**340.5**	On the border	0.99	0.99
P_5		375.4	0	**340.5**	375.4	0	**340.5**	On the border	0.99	0.99
P_6		100	3000	**340.5**	100	3000	**340.5**	Inside of stab. region	1.38	1.38
P_7		300	6000	**340.5**	300	6000	**340.5**	Out of stab. region	0.65	0.65
P_8	Fig. 9, location with	0	**2116.9**	1273.3	0	**2164.5**	1276.8	On the border	1.00	0.99
P_9	respect to the curve	100	**2116.9**	1054.3	100	**2164.5**	1047.7	On the border	0.99	0.99
P_{10}	$q = q_{\text{cr}}/4 * 1$	200	**2116.9**	682.6	200	**2164.5**	673.7	On the border	0.99	0.99
P_{11}		300	**2116.9**	165.5	300	**2164.5**	154.7	On the border	0.99	0.99
P_{12}		325.3	**2116.9**	0	327.1	**2164.5**	0	On the border	0.99	0.99
P_{13}		100	**2116.9**	600	100	**2164.5**	600	Inside of stab. region	1.33	1.32
P_{14}		300	**2116.9**	1000	300	**2164.5**	1000	Out of stab. region	0.72	0.72
P_{15}	Fig. 10, location with	**108.3**	0	1276.8	**108.3**	0	1276.8	On the border	0.99	0.99
P_{16}	respect to the curve	**108.3**	1000	1180.2	**108.3**	1000	1180.2	On the border	0.99	0.99
P_{17}	$M = M_{\text{cr}}/4 * 1$	**108.3**	3000	875.7	**108.3**	3000	878.0	On the border	0.99	0.99
P_{18}		**108.3**	5000	416.3	**108.3**	5000	430.4	On the border	0.99	0.98
P_{19}		**108.3**	6390. 1	0	**108.3**	6498.1	0	On the border	0.99	0.97
P_{20}		**108.3**	3000	400	**108.3**	3000	400	Inside of stab. region	1.30	1.30
P_{21}		**108.3**	6000	800	**108.3**	6000	800	Out of stab. region	0.77	0.77

estimation φ prior to determination of u brings more precise results in comparison with another approach (Table 1).

3.2. *Accuracy of the expressions for an* I*-profile beam*

In order to analyze the accuracy of the expression (42) for I-profile beam, a thin-walled beam with parameters and geometry, which were given previously in Sec. 3 (for Case 1), is considered. Similarly, in the case of individual loading, the critical values according to Eq. (42) are as follows: $M_{\rm cr} = 1801.3\,{\rm N\,m}$, $F_{\rm cr} = 9796.7\,{\rm N}$, $q_{\rm cr} = 1813.3\,{\rm N/m}$ (with $c = 0$). Numerial analysis is carried out with $\alpha = 0.5$, $c = h/2$. The obtained results are presented in Table 2 and Figs. 11–13.

Calculation yields the results as follows:

- 15 sets (M, q, F) being on the border of the stability region (P_{22}–P_{26}, P_{29}–P_{33}, and P_{36}–P_{40}), which are obtained from the expression (42), with safety factor $n_{\rm stab} \approx 1$.
- three sets being inside of the stability region (P_{27}, P_{34} and P_{41} in Figs. 11–13) with $n_{\rm stab} > 1$.
- three sets being outside of the stability region (P_{28}, P_{35} and P_{42} in Figs. 11–13) with $n_{\rm stab} < 1$.

Table 2. Stability safety factor of an I-profile thin-walled ($\alpha = 0.5$, $c = h/2$).

		Parameter set (M, q, F) obtained from the expression (42) or from the graph				Ansys
	Test points	M[N m]	q[N/m]	F[N]	Point location	$n_{\rm stab}$
P_{22}	Fig. 11, location with	0	1602.2	**4898.3**	On the border	0.95
P_{23}	respect to the curve	300	1230.3	**4898.3**	On the border	0.95
P_{24}	$F = F_{\rm cr}/4 * 2$	600	854.8	**4898.3**	On the border	0.95
P_{25}		900	476.1	**4898.3**	On the border	0.95
P_{26}		1273.7	0	**4898.3**	On the border	0.95
P_{27}		400	500	**4898.3**	Inside of stab. region	1.27
P_{28}		1000	1500	**4898.3**	Out of stab. region	0.63
P_{29}	Fig. 12, location with	0	**1071.9**	7800	On the border	0.96
P_{30}	respect to the curve	285.7	**1071.9**	6000	On the border	0.95
P_{31}	$q = q_{\rm cr}/4 * 2$	530.6	**1071.9**	4000	On the border	0.95
P_{32}		735.8	**1071.9**	2000	On the border	0.96
P_{33}		916.0	**1071.9**	0	On the border	0.97
P_{34}		200	**1071.9**	4000	Inside of stab. region	1.16
P_{35}		800	**1071.9**	6000	Out of stab. region	0.75
P_{36}	Fig. 13, location with	**900.6**	0	7347.5	On the border	0.96
P_{37}	respect to the curve	**900.6**	285.3	6000	On the border	0.96
P_{38}	$M = M_{\rm cr}/4 * 2$	**900.6**	611.3	4000	On the border	0.95
P_{39}		**900.6**	871.4	2000	On the border	0.96
P_{40}		**900.6**	1090.2	0	On the border	0.97
P_{41}		**900.6**	500	2000	Inside of stab. region	1.15
P_{42}		**900.6**	600	6000	Out of stab. region	0.85

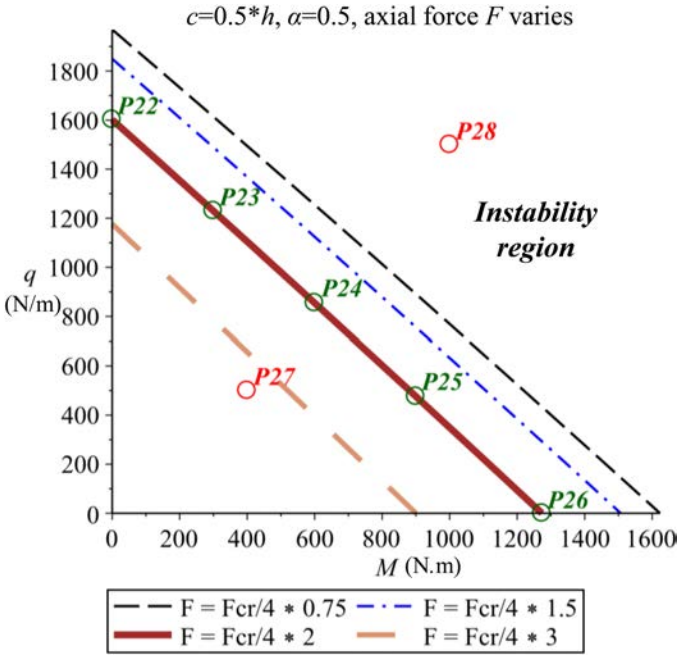

Fig. 11. Boundary of stability region of an I-profile thin-walled beam with variation of axial force F.

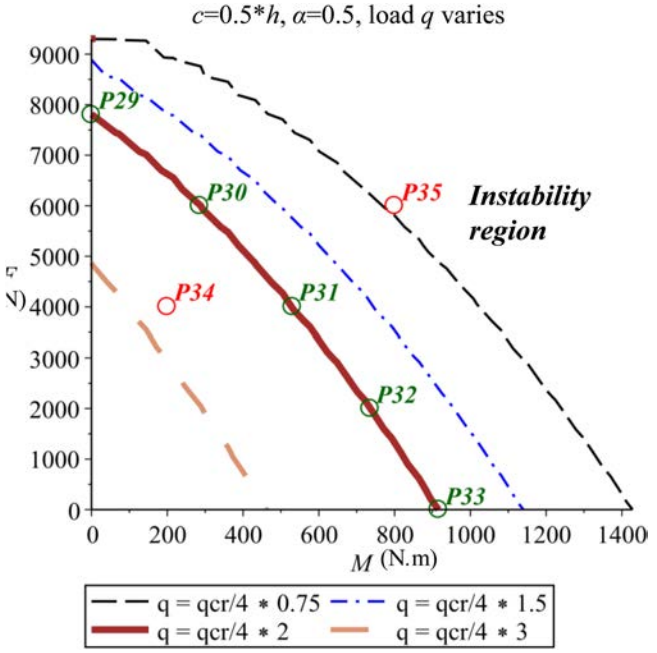

Fig. 12. Boundary of stability region of an I-profile thin-walled beam with variation of uniform distributed load q.

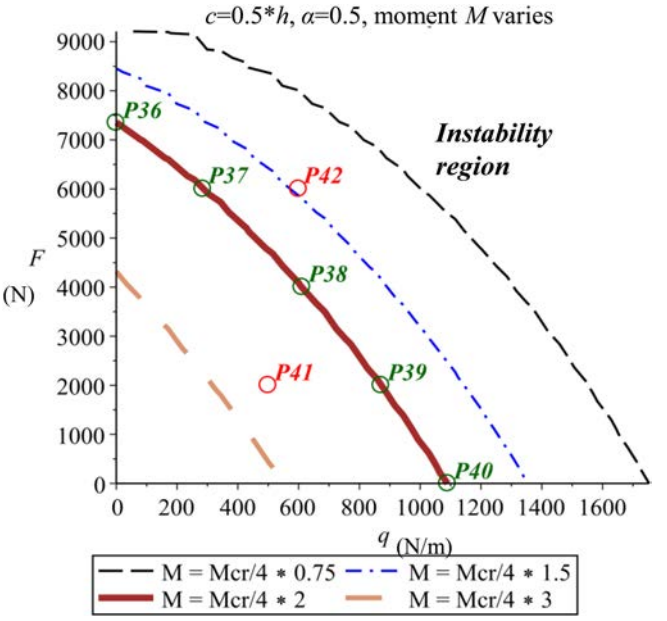

Fig. 13. Boundary of stability region of an I-profile thin-walled beam with variation of moment M.

4. Conclusion

In this paper, a generalized procedure has been improved for determining the critical state of a thin-walled beam under combined symmetric loads. Based on the procedure, the stability issue of the beam under three types of loading was analyzed deliberately with two significant cases: the first one was the beam subjected to axial force F, bending moment M, and concentrated load P, and for the second, load P was replaced by a uniform partial distributed load q. The extraordinary point is when the effect length of q approaches zero, based on the obtained outcome in the second case, it is possible to yield result of the first case.

The effect of load P or q application height on the stability state of the system was also studied. It showed that the higher position of load application (P or q), the higher probability the beam turned to be unstable and vice versa.

The obtained results actually represented a comprehensive form of the outcomes described in the previous publication; subsequently, they play an important role in defining critical load for different cases. The ability to illustrate the outcomes visually in graphical form is quite useful for stability analysis of thin-walled beams in practice. Also, these algebraic equations can make a firm basis for the optimal design. An accuracy of the generalized expression was in agreement with the individual cases in thin-walled beam stability theory, as well as with numerical results from FEM-based software.

Last but not the least, the outcome from two loading cases indicates that the proposed generalized procedure is efficient and easy to implement, particularly it is

also applicable for dealing with the stability problem of thin-walled beams under more complex loading conditions.

Acknowledgment

The authors would like to express the gratitude to the scientists and colleagues at Le Quy Don Technical University, Vietnam and Bauman Moscow State Technical University, Russia for the interest and invaluable scientific contributions to the paper.

Appendix A

A.1. *Constants m_1 and m_2 in Eq.* (14)

$$m_1 = \frac{L^2P(-B_2^{3/2}\pi^2\sin(k) - FL^2\sqrt{B_2}\sin(k) + 2B_2L\sqrt{F}\pi)}{2H^2\sqrt{F}\cos(k)};$$

$$m_2 = \frac{L^2P(B_2\pi^2 + FL^2)\sqrt{B_2}}{2H^2\sqrt{F}};$$

Parameters in Eqs. (35) and (36)

$$u_{11} = \frac{qL^2}{2H};$$

$$u_{12} = -\frac{2L^3qB_2\pi}{H^2};$$

$$\begin{aligned} u_{13} = \frac{L^2}{8\cdot H^3}\cdot(&-\pi^4B_2^2L^2\alpha^2q + 2B_2\pi^2L^4F\alpha^2q - F^2L^6\alpha^2q + 2\pi^4B_2^2\alpha qL^2 \\ &- 4B_2\pi^2L^4F\alpha q + 2F^2L^6\alpha q + 24B_2^2\pi^2L^2q + 8\pi^4B_2^2M \\ &+ 8B_2FL^4q - 16B_2\pi^2L^2FM + 8F^2L^4M) \end{aligned}$$

$$u_{21} = \frac{L^3\alpha q}{2H};$$

$$u_{22} = -\frac{(4M + \alpha qL^2)L^2}{4H};$$

$$u_{23} = \frac{-B_2L^4\pi\alpha q}{H^2};$$

$$\begin{aligned} c_1 = \frac{B_2qL^3}{\cos(k)\sqrt{F}H^3}\cdot\Big(&3B_2L\pi^2\sin(k)\sin(\alpha k)\cos\left(\frac{\alpha\pi}{2}\right)\sqrt{F} \\ &+ 3B_2L\pi^2\cos(\alpha k)\cos(k)\cos\left(\frac{\alpha\pi}{2}\right)\sqrt{F} - B_2^{3/2}\pi^3\sin(k)\sin\left(\frac{\alpha\pi}{2}\right)\cos(\alpha k) \\ &+ B_2^{3/2}\pi^3\sin\left(\frac{\alpha\pi}{2}\right)\cos(k)\sin(\alpha k) + F^{3/2}L^3\sin(k)\sin(\alpha k)\cos\left(\frac{\alpha\pi}{2}\right) \end{aligned}$$

$$+ F^{3/2}L^3\cos(\alpha k)\cos(k)\cos\left(\frac{\alpha\pi}{2}\right) - 3FL^2\pi\sin(k)\sin\left(\frac{\alpha\pi}{2}\right)\cos(\alpha k)\sqrt{B_2}$$
$$+ 3FL^2\pi\sin\left(\frac{\alpha\pi}{2}\right)\cos(k)\sin(\alpha k)\sqrt{B_2} + B_2L\pi^3\alpha\sqrt{F} - F^{3/2}L^3\pi\alpha\Big);$$

$$c_2 = 0;$$

$$c_3 = \frac{L^3qB_2}{\cos(k)\sqrt{F}H^3}\cdot\Big\{3B_2L\pi^2\sin(k)\sin(\alpha k)\cos\left(\frac{\alpha\pi}{2}\right)\sqrt{F}$$
$$- B_2^{3/2}\pi^3\sin(k)\sin\left(\frac{\alpha\pi}{2}\right)\cos(\alpha k) + F^{3/2}L^3\sin(k)\sin(\alpha k)\cos\left(\frac{\alpha\pi}{2}\right)$$
$$- 3FL^2\pi\sin(k)\sin\left(\frac{\alpha\pi}{2}\right)\cos(\alpha k)\sqrt{B_2} + B_2L\pi^3\alpha\sqrt{F} - F^{3/2}L^3\pi\alpha\Big\};$$

$$c_4 = -\frac{B_2qL^3}{\sqrt{F}H^3}\cdot\Big\{3B_2L\pi^2\cos\left(\frac{\alpha\pi}{2}\right)\sin(\alpha k)\sqrt{F} - B_2^{3/2}\pi^3\sin\left(\frac{\alpha\pi}{2}\right)\cos(\alpha k)$$
$$+ F^{3/2}L^3\cos\left(\frac{\alpha\pi}{2}\right)\sin(\alpha k) - 3FL^2\pi\sin\left(\frac{\alpha\pi}{2}\right)\cos(\alpha k)\sqrt{B_2}\Big\}$$

Coefficients R_i in Eq. (42):

$$R_1 = \sqrt{B_2}\cos(k)(T_1 + T_2 + T_3 + T_4 + T_5),$$
$$R_2 = -30B_2^2L^9\sqrt{F}\pi^3\cos(k)\sin(k\alpha)q^2\Big(\cos\left(\frac{\alpha\pi}{2}\right)^2(B_2\pi^2 + FL^2)(B_2^2\pi^4$$
$$+ 14B_2FL^2\pi^2 + F^2L^4) - B_2\pi^2(B_2\pi^2 + 3FL^2)^2\Big),$$
$$R_3 = 60FL^{10}B_2^{5/2}\pi^4\cos(k)\sin(\alpha\pi)\cos(k\alpha)^2q^2(3B_2\pi^2 + FL^2)(B_2\pi^2 + 3FL^2),$$
$$R_4 = 60B_2^2L^9\sqrt{F}q^2\Big[\Big(\cos\left(\frac{\alpha\pi}{2}\right)\Big)^2(B_2\pi^2 + FL^2)(B_2^2\pi^4 + 14B_2FL^2\pi^2 + F^2L^4)$$
$$- B_2\pi^2(B_2\pi^2 + 3FL^2)^2\Big]\sin(k)\pi^3(\cos(k\alpha))^2,$$
$$R_5 = -60B_2^2L^{11}\pi^3F^{3/2}q^2\Big[\Big(\cos\left(\frac{\alpha\pi}{2}\right)\Big)^2(3B_2\pi^2 + FL^2)^2 + \pi^2\alpha^2H^2\Big]\sin(k),$$
$$R_6 = 30FL^{10}\pi^4B_2^{5/2}\sin(\alpha\pi)\sin(k)\sin(k\alpha)q^2(3B_2\pi^2 + FL^2)(B_2\pi^2 + 3FL^2),$$
$$R_7 = -120B_2^2L^{11}\pi^4F^{3/2}\cos\left(\frac{\alpha\pi}{2}\right)\sin(k\alpha)\alpha q^2(3B_2\pi^2 + FL^2)H,$$
$$R_8 = 120FL^{10}\sin\left(\frac{\alpha\pi}{2}\right)\cos(k\alpha)\pi^5B_2^{5/2}\alpha q^2(B_2\pi^2 + 3FL^2)H,$$

where

$$T_1 = -60L^4\pi^2cqH^6\sin\left(\frac{\alpha\pi}{2}\right);$$
$$T_2 = \frac{15}{2}L^6q\sin(\alpha\pi)\cdot\Big\{\frac{1}{4}B_2L^2\pi^4\alpha q(\alpha-1)(B_2^4\pi^8 - 5B_2^3FL^2\pi^6 + 10B_2^2F^2L^4\pi^4$$
$$- 10B_2F^3L^6\pi^2 + 5F^4L^8) - M\pi^2H^5 - \frac{3}{4}B_2L^2\pi^2q(B_2^4\pi^8 + 15B_2^3FL^2\pi^6$$
$$+ 50B_2^2F^2L^4\pi^4 + 22B_2F^3L^6\pi^2 - 3F^4L^8) - \frac{1}{4}F^5L^{12}q(\pi^2\alpha^2 - \pi^2\alpha + 1)\Big\};$$

$$T_3 = \frac{15}{8}L^8\pi\alpha q^2 H(3B_2^4\pi^8 - 40B_2^3FL^2\pi^6 - 90B_2^2F^2L^4\pi^4 - F^4L^8)\cos(\alpha\pi);$$

$$T_4 = 120B_2^2FL^{10}\pi^5\alpha q^2(B_2\pi^2 + 3FL^2)H\left(\cos\left(\frac{\alpha\pi}{2}\right)\right)^2;$$

$$\begin{aligned}T_5 = {} & \pi^3H^5\pi^2\left(-\frac{1}{8}L^8\alpha^5q^2 + \frac{5L^8\alpha^4q^2}{16} + 15B_2CL^2\pi^2 + 15B_2DD\pi^4 - 15CFL^4\right.\\ & \left. - 15DDFL^2\pi^2 - 15L^4M^2\right) - \frac{\pi^3H^515L^6qM(\pi^2+2)\alpha}{4} + \pi^3H^3\\ & \times\left[\frac{5}{4}L^6q\alpha^3(B_2^2M\pi^6 + 2FL^4q(3B_2\pi^2 + FL^2) - 2FL^2M\pi^2(B_2\pi^2 - 1/2FL^2))\right.\\ & \left. - \frac{1}{16}(5L^8q^2\alpha^2(F^2(\pi^2+12)L^4 - 2FB_2\pi^2(\pi^2-18)L^2 + B_2^2\pi^6))\right]\\ & - 15\pi^3L^{10}q^2B_2F(9B_2^2\pi^4 + 22B_2FL^2\pi^2 + F^2L^4)\alpha H.\end{aligned}$$

Coefficients S_i in Eq. (50):

$$\begin{aligned}S_1 = {} & -L^8\left\{15(\pi^4\alpha^4 - 2\pi^4\alpha^3 + \pi^4\alpha^2 + 84\pi^2\alpha^2 - 110\pi^2\alpha - 826)\sin(\alpha\pi)\right.\\ & - 30\pi(\pi^2\alpha^3 - 7\pi^2\alpha^2 + 6\pi^2\alpha - 221\alpha + 96)\cos(\alpha\pi)\\ & + 960\alpha\pi(\pi^2\alpha^2 - \pi^2\alpha - 12)\sin\left(\frac{\alpha\pi}{2}\right) + 5760\pi^2\alpha^2\cos\left(\frac{\alpha\pi}{2}\right)\\ & \left. + 7\pi^5\alpha^5 - 20\pi^5\alpha^4 + 15\pi^5\alpha^3 + 500\pi^3\alpha^3 + (180\pi^3 + 5760\pi)\alpha + 2880\pi\right\}\end{aligned}$$

$$\begin{aligned}S_2 = {} & 40L^6\pi^2\left[3(\pi^2\alpha^2 - \pi^2\alpha + 7)\sin(\alpha\pi) + 3\pi(\alpha+4)\cos(\alpha\pi)\right.\\ & \left. + 48\alpha\pi\sin\left(\frac{\alpha\pi}{2}\right) + 2\pi^3\alpha^3 - 3\pi^3\alpha^2 - 24\alpha\pi - 12\pi\right],\end{aligned}$$

$$\begin{aligned}S_3 = {} & -L^6C\pi^2\left\{30(-\pi^2\alpha^2 + \pi^2\alpha - 33)\sin(\alpha\pi) + 30\pi(\alpha-8)\cos(\alpha\pi)\right.\\ & - 1920\alpha\pi\sin\left(\frac{\alpha\pi}{2}\right) + 2\pi^5\alpha^5 - 5\pi^5\alpha^4 - 120\pi^3\alpha^3\\ & \left. + 5\pi^3\alpha^2(\pi^2+36) + 960\alpha\pi + 240\pi\right\},\end{aligned}$$

$$S_4 = -240L^4\pi^4(\sin(\alpha\pi) + \alpha\pi),$$

$$S_5 = -20L^4C\pi^4[6\sin(\alpha\pi) - \pi^3\alpha^3 + 3\pi(\pi^2+2)\alpha],$$

$$S_6 = -240\pi^7L^2C,$$

$$S_7 = -240L^2\pi^7C^2,$$

$$S_8 = 240B_2\pi^9C^2.$$

References

1. S. Timoshenko and J. M. Gere, *Theory of Elastic Stability*, 2nd edn. (McGraw-Hill, New York, 1961).
2. V. Z. Vlasov, *Tonkostennye uprugie sterzhni (Thin-Walled Elastic Beams*), 2nd edn. (Fizmatgiz, Moscow (in Russian), 1959).
3. N. A. Alfutov, *Stability of Elastic Structures* (Springer, Berlin, 2000).
4. Z. P. Bazant and L. Cedolin, *Stability of Structures* (World Scientific Publishing, Singapore, 2010).
5. B. Kim, L. Y. Li and A. Edmonds, Analytical solutions of lateral–torsional buckling of castellated beams, *Int. J. Struct. Stab. Dyn.* **16**(8) (2016) 1550044.
6. Z. Chen, J. Li and L. Sun, Calculation of critical lateral torsional buckling loads of beams subjected to arbitrarily transverse loads, *Int. J. Struct. Stab. Dyn.* **19**(3) (2019) 1950031.
7. M. Shama, *Buckling of Ship Structures* (Springer, Berlin, 2013).
8. J. Wu, Q. H. Cheng, B. Liu, Y. W. Zhang and K. C. Hwang, Study on the axial compression buckling behaviors of concentric multi-walled cylindrical shells filled with soft materials, *J Mech. Phys. Solids* **60**(5) (2015) 803–826.
9. H. C. Bui, Buckling analysis of thin-walled sections under general loading conditions, *Thin-Walled Struct.* **47** (2009) 730–739.
10. M. A. Bradford and X. Liu, Flexural-torsional buckling of high-strength steel beams, *J. Construct. Steel Res.* **124** (2016) 122–131.
11. F. Mohri, N. Damil and M. Potier-Ferry, Review and comparison of finite element flexural–torsional models for non-linear behaviour of thin-walled beams, *Adv. Eng. Softw.* **80** (2015) 174–187.
12. M. Bajer, J. Barnat and J. Pijak, Lateral torsional buckling of selected cross-section types, *Proc. Eng.* **190** (2017) 106–110.
13. A. Y. T. Leung, Dynamics and buckling of thin pre-twisted beams under axial load and torque, *Int. J. Struct. Stab. Dyn.* **10**(5) (2010) 957–981.
14. X. T. Chu, Z. M. Ye, L. Y. Li and R. Kettle, Local and distortional buckling of cold-formed zed-section beams under uniformly distributed transverse loads, *Int. J. Mech. Sci.* **48** (2006) 378–388.
15. E. Madenci and I. Guven, *The Finite Element Method and Applications in Engineering Using ANSYS* (Springer, New York, 2015).
16. Y. Nakasone, S. Yoshimoto and T. A. Stolarski, *Engineering Analysis with ANSYS Software* (Elsevier, Oxford, 2006).
17. P. Goncharov, I. Artamonov and T. Khalitov, *Engineering Analysis with NX Advanced Simulation* (Lulu Press, North Carolina, 2014).
18. R. F. Vieira, F. B. E. Virtuoso and E. B. R. Pereira, Buckling of thin-walled structures through a higher order beam model, *Comp. Struct.* **180** (2017) 104–116.
19. I. Pesic, D. Lanc and G. Turkalj, Non-linear global stability analysis of thin-walled laminated beam-type structures, *Comp. Struct.* **173** (2016) 19–30.
20. Y. L. Xu, Y. J. Shi, Y. R. Wu and H. Y. Ban, Experimental and numerical study on lateral-torsional buckling behavior of high performance steel beams, *Int. J. Struct. Stab. Dyn.* **18**(8) (2018) 1850090-1-29.
21. F. Mohri, C. Bouzerira and M. Potier-Ferry, Lateral buckling of thin-walled beam-column elements under combined axial and bending loads, *Thin-Walled Struct.* **46** (2008) 290–302.
22. F. Mohri, N. Damil and M. Potier-Ferry, Buckling and lateral buckling interaction in thin-walled beam-column elements with mono-symmetric cross sections, *Appl. Math. Model.* **37** (2013) 3526–3540.

23. S. S. Cheng, B. Kim and L. Y. Li, Lateral–torsional buckling of cold-formed channel sections subject to combined compression and bending, *J. Construct. Steel Res.* **80** (2013) 174–180.
24. T. Yilmaz and N. Kirac, Analytical and parametric investigations on lateral torsional buckling of European IPE and IPN beams, *Int. J. Steel Struct.* **17**(2) (2017) 695–709.
25. N. Challamel, Lateral-torsional buckling of beams under combined loading: A reappraisal of Papkovitch–Schaefer theorem, *Int. J. Struct. Stab. Dyn.* **7**(1) (2007) 55–79.
26. E. Magnucka-Blandzi, Critical state of a thin-walled beam under combined load, *Appl. Math. Model.* **33** (2009) 3093–3098.
27. E. Magnucka-Blandzi and K. Magnucki, Buckling and optimal design of cold formed beams; reviews of selected problems, *Thin-Walled Struct.* **46** (2011) 554–561.
28. A. Osmani and S. A. Meftah, Lateral buckling of tapered thin walled bi-symmetric beams under combined axial and bending loads with shear deformations allowed, *Eng. Struct.* **165** (2018) 76–87.
29. P. Van Binh, D. Hoang Minh, G. Sergei Sergeevich and N. Viet Duc, Boundary of stability region of a thin-walled beam under complex loading condition, *Int. J. Mech. Sci.* **122** (2017) 355–361.
30. H. Ozbasaran, Optimal design of I-section beam-columns with stress, non-linear deflection and stability constraints, *Eng. Struct.* **171** (2018) 385–394.
31. H. Ozbasaran and T. Yilmaz, Shape optimization of tapered I-beams with lateral-torsional buckling, deflection and stress constraints, *J. Construct. Steel Res.* **143** (2018) 119–130.
32. K. Magnucki, Some problems of optimization of beam and shell structures under elastic stability constraints, Dissertation, Poznan University of Technology (in Polish) (1993).